Published in final edited form as:
J Surg Oncol. 2011 May 1; 103(6): 475–483. doi:10.1002/jso.21794.

Experimental Models to Study Lymphatic and Blood Vascular Metastasis

Lu Chen, MD, PhD[1], **Byron Hann, MD, PhD**[2], and **Lily Wu, MD, PhD**[3]

[1]Center for Eye Disease & Development, Program in Vision Science and School of Optometry, University of California, Berkeley, California

[2]Helen Diller Family Comprehensive Cancer Center, University of California at San Francisco, San Francisco, California

[3]Department of Molecular & Medical Pharmacology, Institute of Molecular Medicine, University of California, Los Angeles, California

Abstract

As a model system for the understanding of human cancer, the mouse has proved immensely valuable. Indeed, studies of mouse models have helped to define the nature of cancer as a genetic disease and demonstrated the causal role of genetic events found in tumors. As an experimental platform, they have provided critical insight into the process of tumor metastasis in the lymphovascular system. Once viewed with skepticism, mouse models are now an integral arm of basic and clinical cancer research. The use of a genetically tractable organism that shares organ systems and an immense degree of genetic similarity to humans provides a means to examine multiple features of human disease. Mouse models enable development and testing of new approaches to disease prevention and treatment, identification of early diagnostic markers and novel therapeutic targets, and an understanding of the in vivo biology and genetics of tumor initiation, promotion, progression, and metastasis. This review summarizes recent mouse models for lymphangiogenesis and the process of lymphovascular metastasis, focusing on the use of the cornea as an experimental platform for lymphangiogenesis in inflammation and immunity, and on the use of molecular and viral vector mediated imaging and to identify and monitor lymph node metastases of prostate cancer.

I. CORNEAL MODELS TO STUDY THE LYMPHATIC PATHWAY

Lu Chen, MD, PhD

Introduction

The cornea is the forefront tissue in the visual pathway, which provides a clear structure for the passage of light. It is also one of few tissues in the body that are normally devoid of any vascular structures, blood, or lymphatic. Also due to its transparent nature and accessible location, the cornea has been extensively exploited as a tool to study hemangiogenesis. It is estimated by Dr. Judah Folkman, the founder and grandfather of tumor hemangiogenesis research, that more than one-third of our basic knowledge on blood vessels is derived from the studies with the cornea during the past few decades. More recently, the use of this unique tissue in lymphatic research, a field of new discovery [1–7], has attracted broad attention and started to generate considerable amount of promising data [1]. This paper reviews current corneal models used for lymphatic studies in recent years.

Correspondence to: Byron Hann.

Model Systems—Generally speaking, the corneal models recently used for lymphatic studies fall into two major categories: the lymphangiogenesis models which have been used to investigate the processes and mechanisms of lymphatic vessel formation and regulation, and the transplantation models which have been exploited to study the specific roles of the lymphatic pathway in immune responses.

Lymphangiogenesis models. It has been known for decades that lymphatic vessels are induced into the alymphatic corneas after pathological stimulations [8,9]. However, since the lymphatics are not easily visible as blood vessels, their identification is heavily relied on the anatomical ultrastructural features in earlier studies. This technical limitation has greatly hampered the progression of lymphatic research, leading to a historical negligence for decades. With the recent discovery of several lymphatic specific molecules and the advancement of modern biology and imaging technologies, corneal lymphatic research has been re-ignited during the past few years with a great advancement of our knowledge at both molecular and cellular levels [1–7,10].

The most commonly used corneal model to study inflammatory lymphangiogenesis is the suture placement model where fine surgical sutures are placed into the corneal stroma without penetrating into the anterior chamber [1,11,13–15]. The time course and distribution pattern of corneal lymphangiogenesis induced by suture placement in mice have been well defined to produce highly reliable and replicable data, which can be analyzed by computerized image analysis programs, such as the NIH Image J software. Most recently, it has also been found that the lymphatic distributions in mouse corneas vary among different strains and between the nasal and temporal sides [15]. Compared with the BALB/c mice, the C57BL/6 mice demonstrate a higher baseline level of lymphatic coverage in normal limbal areas. Both strains adopt a nasal dominant distribution pattern of lymphatic vessels under normal and inflamed conditions, which is not observed for blood vessels [15].

Another well-defined model for corneal lymphangiogenesis study is the micropocket assay, which is accomplished by inserting a material of interest into a small intrastromal space created by a surgical knife. This assay was first introduced by Folkman's group in the early 1970s for hemangiogenesis research [16,17]. Recently, it has been adapted for lymphatic investigation [5,18]. The obvious advantage of this model is that it can test one material of particular interest, whether it is in the form of a growth factor, a cell suspension, or a tumor tissue [14,18–20]. This model also generates highly predictable and reproducible results, particularly after the introduction of slow-releasing pellets with no inflammatory stimulus [21–23]. Though still at its pioneering phase, it is reasonable to believe that lymphatic research using this micropocket assay is destined for continued success. For more than 30 years, this model has served as one of the best and cleanest in vivo systems for evaluating pro-and anti-hemangiogenesis factors and mechanisms.

Other corneal models for lymphatic studies include the chemical burn and trauma models, which were less frequently reported [24,25]. It is also worth noting that the normal alymphatic cornea itself provides an ideal model to study anti-lymphangiogenesis factors and mechanisms. For example, using this alymphatic tissue by nature, it was recently discovered that an alternatively spliced vascular endothelial growth factor receptor-2 (sVEGFR-2) is an endogenous lymphatic inhibitor which is also expressed in other tissues. The administration of sVEGFR-2 demonstrates a suppression effect on lymphangioma cellular proliferation [26]. In addition to the above-mentioned models, a number of transgenic or knockout mice have also been exploited for corneal lymphatic studies [14,26–28], reflecting another forefront of research effort.

Transplantation models. The corneal transplantation model provides a clear demonstration of cell trafficking from the cornea to draining lymph nodes which is afforded by lymphatic channels. The surgery is performed for replacing the central cornea of the recipient with a donor cornea button [27,29]. Briefly, the immune reflex arc in corneal transplantation consists of the following components: (i) the afferent pathway of lymphatic vessels through which antigens and antigen presenting cells migrate to the draining lymph nodes, (ii) the lymph nodes where T cell priming occurs, and (iii) the efferent pathway of blood vessels through which the primed T cells are homed to the targeted corneal grafts [1]. The critical role of the lymphatic pathway in corneal transplantation immunity has been demonstrated in mice that surgical severing of the lymphatic pathway leads to universal graft survival [30]. More recent data have also revealed a variety of molecules or factors that are critically involved in the lymphatic pathway and transplantation immunity in mice [1], among which is VEGFR-3, an emerging target for cancer therapy [13].

Another advantage of this model is that the transplantation surgery can be performed on the normal (alymphatic; low-risk setting) or the inflamed (lymphatic-rich; high-risk setting) corneas with differentiable outcomes. While the low-risk grafts enjoy a high rate of survival, a majority of the high-risk grafts end up on the rejection list. These low-risk and high-risk models therefore provide an excellent tool to differentiate lymphatic responses and their specific roles in normal and inflamed conditions. Using these models, it has been demonstrated that in the high-risk setting, the trafficking of donor-derived cells to the recipient draining lymph nodes is greatly enhanced, compared to the low-risk setting [29]. Finally and yet to be explored, the transplantation model can also be used to study the cellular mechanisms of lymphatic vessel formation since either the donor-or recipient-derived cells can be labeled and tracked before or after the transplantation procedure.

Conclusions—The cornea provides an ideal tissue for lymphatic research. The list of corneal models will keep expanding as more investigations are carried out in this rapidly growing field. As proven in the past to be a powerful model for hemangiogenesis studies, the cornea will continue to provide an excellent site for lymphatic research to develop novel therapeutic strategies to combat lymphatic diseases, both inside and outside the eye.

II. GENE EXPRESSION-BASED MOLECULAR IMAGING TO DETECT NODAL METASTASIS OF PROSTATE CANCER

Lily Wu, PhD

The availability of a specific, non-invasive imaging modality to detect lymph node metastasis is critical to the management of many solid tumors, as nodal involvement is a poor prognostic indicator. We developed a molecular imaging strategy to detect nodal metastases of prostate cancer and breast cancer by using recombinant adenoviral vectors. This technology takes advantage of the innate lymphotropic properties of adenovirus in conjunction with the tumor-or tissue-restricted expression of imaging reporter genes that were incorporated in the vector. The imaging signals produced by the cell-specific vector correlated with the presence of metastatic lesions in the draining lymph nodes of breast and prostate cancer models. This method could enable the use of clinical imaging modality such as positron emission tomography (PET) to directly identify involved nodes without lymph node sampling and histological analysis. Moreover, this gene expression-based functional imaging could be tailored to detect nodal metastasis based on the transcriptionally upregulated genetic program in each tumor.

Molecular Imaging of Prostate Cancer in Clinical Settings

Treatment decisions in a patient with malignant tumor are dependent on the stage of the disease. The oncological team will use physical examination, imaging, and pathology at biopsy, to determine whether a cancer is localized, locally advanced with high risk of future metastasis, or already metastatic. Based on the pre-treatment evaluation and the natural history of each cancer, there follows a local treatment (typically radiotherapy or surgery), a systemic treatment (often chemotherapy or hormonal deprivation therapy), or a combination of these. For most cancers, the status of the lymph nodes is of prime importance in the treatment decision-making process as the spread of cancer cells to regional lymph nodes through the lymphatic vasculature is the first step in metastatic dissemination, which carries a poor prognostic indication [31,32]. This is the case for prostate cancer, the most common malignancy in American men with newly diagnosed cases of over 200,000 per year.

Conventional imaging modalities such as computed tomography (CT) and magnetic resonance imaging (MRI) are useful in evaluating anatomical and structural abnormalities such as size and shape. However, the ability to detect small volume tumor or nodal involvement in the absence of adenopathy is poor. The recent development of an iron oxide paramagnetic nanoparticle as a MRI contrast agent identifies tumor-infiltrated region within lymph nodes based on the lack of contrast signal in the infiltrated regions [33]. This technology does not identify the presence of tumor cells directly, but rather it relies upon nodal infiltration of macrophages that have engulfed the magnetic particles. Nodal regions occupied by metastatic lesions would be inaccessible to macrophages. PET is an imaging modality that uses radiolabeled tracer to query the metabolic and biological activity of diseases. The most widely used PET tracer in oncology is the glucose analogue 2-deoxy-2-[F-18] fluoro-$_{D}$-glucose (FDG). In comparison to normal or resting tissues, the metabolism of cancer cells is highly dependent on anaerobic glycolysis rather than oxidative phosphorylation as first observed by German biochemist Otto Warburg in 1924. Recent studies revealed that the shift in cellular metabolism to aerobic glycolysis in cancer cells is due to the switch to a M2 isoform of pyruvate kinase, distinct from the M1 isoform in normal cells [34]. The greatly heightened glucose uptake [35] and metabolism in cancer cells have enabled the wide application of whole body FDG-PET scan in cancer detection and treatment monitoring. Increased glucose metabolism is, however, not unique to malignant tissue. Benign tumors, inflammatory conditions, and normal tissue under physiological exertion can all exhibit increased rate of glucose metabolism and produce false positive signals. The advent of combined PET and CT imaging (PET/CT) devices 10 year ago enables the simultaneous acquisition of biologic and anatomic data in one examination [36]. The correct assignment of biological abnormalities in the context of anatomic landmarks with PET/CT has been helpful in resolving some of the false positive issues of FDG-PET in oncology. These advantages of combined PET/CT modality can be appreciated even in oncology research in the small animal preclinical imaging settings (Fig. 1).

Despite the improved technologies, FDG-PET plays a limited role in the detection and management of prostate cancer. The challenges encounter in imaging the primary tumor include: (i) the excretion of tracer into bladder obscuring the adjacent prostate pathology, (ii) relative low glycolytic activity of localized, well-differentiated prostate cancer [37], and (iii) the overlap of signal intensity with prevalent benign conditions such as prostatic hypertrophy. Even in advanced, metastatic disease the performance of FDG-PET are mixed. As reported by Shreve et al. [38], FDG-PET is less sensitive than bone scan for detecting osseous metastasis, but exhibits a higher positive predictive value of 98% for the presence of metastasis. The detection rate of lymph node metastasis in recurrent prostate cancer with elevated serum prostate-specific antigen (PSA) remained low, positive in 50% of patients [39]. Current on-going research efforts to improve the diagnostic capability of PET/CT for

prostate cancer include the development of more disease-specific tracers such as 16b-18F-fluoro5-dihydrotestosterone (F18-DHT, Ref. [40]) to assess the expression of androgen receptor, an established oncogenic driver and therapeutic target of prostate cancer [41], as well as [F-18]-choline [42] and a synthetic L-leucine analog (anti [F-18]-FACBC) [43] are showing promising results to detect prostate cancer based on its altered cellular membrane and amino acid metabolism, respectively. Moreover, [C11]-choline has proven to be an appropriate tracer for noninvasive imaging of primary prostate tumor as well as nodal and distant metastases (Fig. 2) [44–47]. One advantage of [C-11]-over [F-18]choline is the absence of high urinary excretion, which provides clear PET images of the pelvic lymphatic drainage region. The disadvantage of using [C-11]-choline is its short half life (20 min for C-11, compared to 110 min for F-18), which requires a cyclotron to be located nearby. The experience of using the newer PET tracers so far is limited to clinical studies with a small cohort of patients. Further clinical validation of their imaging sensitivity and specificity in larger populations of prostate cancer patients in the appropriate clinical scenario is needed.

Reporter Gene Imaging

Due to numerous limitations with current modalities to image prostate cancer, especially for those spread to regional lymph nodes or locally advanced, further development to achieve more effective and specific non-invasive imaging for this disease is greatly needed. A fruitful area of molecular imaging research is in the use of “reporter genes” to interrogate and visualize the functional activities of cancer cells in a living subject. The definition of a reporter gene is that it encodes a gene product that readily produces photons that can measure by an imaging instrument. Since most of the reporter gene products are exogenous or engineered proteins, they usually exhibit a low background activity in the host. Due to this reason, reporter gene based imaging promises to achieve high specificity. A list of commonly used imaging reporter genes, each gene’s enabling substrate or tracer, and some of the applications are summarized in Table I. These genes include the bioluminescent reporter firefly luciferase (FL) and renilla luciferase (RL), the fluorescent reporter green fluorescent protein (GFP), red fluorescent protein (RFP), and the recently developed near-infrared fluorescent protein (IFP) [48], the PET reporter gene HSV1thymidine kinase (HSV1-tk) [49], and sodium/iodine symporter (NIS) [50] and the somatostatin receptor SSTR2 [51] for SPECT imaging. The advantages of optical imaging in small animals, especially bioluminescence imaging (BLI), in comparison to PET include high sensitivity, low background, higher throughput, lower cost, and no hazard of radioactivity. However, a key advantage of PET is its ability to achieve quantitative, 3-D localized signal that can be applied to the clinic. A comprehensive coverage of the topic of reporter gene imaging is beyond the scope of this article. Interested readers should consult recent reviews for more detail on this topic [52–54]. Below I will discuss three specific applications of reporter gene imaging relevant to the investigation of prostate cancer metastasis in animal models. These applications include: (i) the use of imaging reporter gene marked tumor models to study metastatic behavior in vivo, (ii) the use of gene regulatory promoters that are cell-or tumor-specific to control the expression of reporter genes to enhance the specificity of imaging, and (iii) the use of adenoviral vector to specifically image the nodal metastasis of prostate cancer.

Imaging Reporter Gene-Marked Tumor Cells

A widely used approach to study metastasis in living animals is to engineer tumor cells to stably express an optical reporter gene such as FL or GFP, which enables the non-invasive, repetitive detection of primary tumors, and disseminated lesions in an individual animal over time. As shown in Figure 3A, the low background activity of luciferase-based BLI makes it a favorable modality for repetitive, longitudinal monitoring of metastasis in the same animal. However, due to light absorption and scattering by tissues, BLI is semi- quantitative

and does not allow 3-D localization of the signal. To overcome this inherent limitation of BLI, we and others use ex vivo imaging of isolated organs to provide better localization and quantification of the signals emanating from the disseminated tumor cells (Fig. 3B). Moreover, in our experience the bioluminescence signal intensity of the isolated organs correlates well with the volume of metastases, as assayed by conventional histological means (Fig. 3C). The BLI approach provides a rapid, lump sum assay of metastatic volume, which saves a significant amount of time and efforts when compared to complete histological analyses of the tissue.

Gene Expression-Based Imaging

Gene expression-based imaging has emerged as a facile and flexible approach for studying signaling pathways during tumor progression in live animals [55]. In this approach, a pathway-or cell-specific promoter is placed upstream of an imaging reporter gene to drive its expression, and this reporter cassette is introduced into tumor cells in a live animal either by the genetically engineered transgenic method or by using viral gene delivery vectors. Several prostate-specific promoters that have been successfully employed to express therapeutic or imaging genes in prostate cancer gene therapy applications [56], included the most commonly utilized PSA promoter [57,58], as well as hK2 [59], rat probasin [60], and chimeric promoters such as the fusion of PSA and PSMA enhancer sequences [61] and fusion of PSMA enhancer/PSA enhancer/T-cell receptor gamma-chain alternate reading frame protein sequences (PPT) [12]. However, the transcriptional potency of tissue-specific promoters is often much weaker in comparison to constitutive viral promoters leading to inefficient expression and limited imaging capability. Hence, our research group has developed an amplification method termed the two-step transcriptional activation (TSTA) system, which activates a strong transcriptional activator that induces an imaging reporter gene [62]. The functionality of the TSTA system is illustrated with a prostate-targeted adenovirus [63,64]. In Figure 4A, the genomic organization of this prostate-specific recombinant adenovirus, AdTSTA-tk, is shown. In this virus, a modified PSA promoter was used to control the expression of the synthetic Gal4VP16 transcription activator, which is composed of the strong VP16 transactivation domain fused to the Gal4 DNA-binding domain (Gal4DBD). Gal4 responsive elements were placed upstream of the promoter that drives the expression of an imaging reporter gene. In doing so, Gal4VP16 protein strongly transactivates the expression of the imaging reporter genes, such as HSV1-tk or the firefly luciferase gene [63–65]. The potency of gene expression of AdTSTA-tk is very comparable to the constitutive cytomegalovirus (CMV) promoter driven vector (AdCMV-tk) in prostate cancer cell lines (Fig. 4B). A clear distinction is that the prostate specificity of AdTSTA-tk enabled the expression of the HSV-tk PET reporter gene in the prostate tumor, but restricted gene expression in non-prostate tissue such as the liver despite the inadvertent gene delivery to this site (Fig. 4C) [64,65]. In principle, the TSTA method can be applied to amplify any pathway-, cell-or tumor-specific promoter. Extensive utilization of this method by our group and others verified that its ability to greatly enhance transcription of a wide range of cancer- and tissue-specific promoters, for example, Survivin, Mucin1, VEGF, and cardiac-specific promoters [66–68].

Viral Vector-Mediated Imaging of Nodal Metastasis

A commonly used method to assess nodal status is the sentinel lymph node biopsy (SLNB). This method is based on the removal of the first draining, or sentinel lymph node (SLN) as determined by lymphatic uptake of radiolabeled colloids or dyes. The current method of intraoperative lymphoscintigraphy entails the use of a gamma camera to monitor the transit of a 99mTc-filtered sulfur colloid particle from the peritumoral injection site into the SLN, which is then harvested for histopathological examination [69]. In developing an ideal lymphoscintography agent to query SLN status, it is important to employ particles that

favorably traffic to and accumulate in the LNs. The size and surface properties of particles are key determinants of their lymphotropic properties [70], and the particles used in clinics typically range in size from 50 to 200 nm [69]. Retention of the particles in the lymph nodes is mainly due to phagocytosis by the macrophages [71], and it has been advocated that the optimal particles size for lymphscintography is 100 nm [69]. Extensive experience in mapping the lymphatic drainage of tumor has come from the melanoma and breast cancer field, where determining the SLN status is a standard part of care [72].

In the clinical management of prostate cancer, there is a general consensus about the importance of lymph node status in patient outcome. However, unlike breast cancer and melanoma, there is no uniform practice to ascertain nodal status of prostate cancer. In patients with prostate cancer, clinical variables including serum PSA levels, Gleason tumor grade, and digital rectal examination are useful in predicting outcome. Among the adverse pathologic features of prostate cancer, the presence of pelvic lymph node metastasis is the strongest predictor of disease recurrence and progression [73–75]. For instance, the 10-year progression-free survival probabilities were 79% for organ confined disease, which decreased to only 12% for disease with nodal involvement [74]. Moreover, recent molecular investigations in preclinical models and clinical cases highlighted the strong association of tumoral lymphangiogenesis, namely the heightened expression of VEGF-C and VEGFR-3, with regional lymph node metastasis [76–79]. Our work further supports that lymphogenous spread can augment systemic metastasis [78,79]. The lymphatic drainage of prostate gland is very complex [80] and a thorough LN sampling within the pelvic region would be a time- and labor-intensive procedure that carries risk of complications such as lymphoceles, lymphedema, and venous thrombosis, with an estimated incidence of 20% [81]. Given the significance of LN status in prostate cancer, it will be valuable to develop an imaging modality that is capable of one-step, direct visualization of nodal metastasis.

Recently, we and others demonstrated the lymphotropic properties of adenovirus, which is likely attributed to its negative surface charge and 100nm size [82–84]. We further postulated that the amplified lymphangiographic approach, nodal metastasis in the pelvic lymph prostate-specific TSTA imaging vectors could be applied in a nodes or axillary lymph nodes was visualized by BLI or PET, lymphangiography approach to detect nodal metastasis of prostate respectively (Fig. 6A,B). By injecting AdTSTA-tk into peritumoral cancer (Fig. 5). In the study by Burton et al. [85], we reported that one-area, akin to the lymphoscintigraphic approach to visualize SLN, step visualization of prostate cancer lymphatic metastasis is feasible micrometastasis of SLN was detected by PET–CT (Fig. 6C). This using the PSA promoter driven TSTA adenoviral vector expressing adenoviral lymphangiographic imaging technology can feasibly query either the luciferase or the HSV-tk imaging reporter gene. By injecting different types of solid tumors. As noted above, a wide range of tissue-the AdTSTA-fl or AdTSTA-tk via the lymphatic rich paws in a and tumor-specific promoters have been successfully adapted to the TSTA gene amplification method and incorporated in adenoviral vectors to target selective types of cancer. We demonstrated that a TSTA vector driven by the tumor-selective Mucin-1 promoter was able to detecting SLN metastasis in an orthotopic breast tumor model [67]. Using a telomerase-dependent replicating adenovirus, Kishimoto et al. [84] demonstrated its feasibility in a fluorescent imaging strategy to detect nodal metastasis of colon cancer and in determining the precise surgical margin [86]. The cell-restricted expression capability of the AdTSTA vector is valuable as systemic-directed vector delivery was successful in detecting metastatic lesions in the lungs, lymph nodes and peritoneum in murine models of prostate and breast cancer [57,67,87] and data not shown.

The gene expression-based imaging approach, we have demonstrated in this review, holds great promise towards the noninvasive direct visualization of nodal metastases. Several

recent reports have demonstrated the safety and feasibility of using adenoviral vector to deliver reporter genes such as HSV-tk and sodium iodine symporter (NIS) to achieve specific imaging signals in hepatic and prostate tumors in patients [88,89]. Despite the gains in concepts and technology, the clinical translation of adenoviral vector based gene delivery is hampered largely by pre-existing host immunogenicity towards human adenoviruses. Hence, the future of vector research will need to include: (i) the detail understanding of viral capsid structure [90]; (ii) the in vivo biodistribution of virus [83] and its interaction with serum factors [91]; (iii) the innovative engineering of viral surface architecture to circumvent pre-existing immunity [92] and to achieve optimal transductional targeting of cancer cells [93]; and (iv) the blunting of the host immune response. Moreover, many of the experiences and technologies gained in viral vectors could be adapted to the burgeoning field of nanotechnology with ever-expanding “smart nanoparticles” that intricately control their payload release. Thanks to the steady gains of significant advancement in vectorology, molecular oncology, and imaging, we foresee the translation of a wide range of transcriptional-targeted reporter gene imaging to clinical oncology practices could be achieved in the near future.

Acknowledgments

This work is supported in part by research grants from National Institutes of Health (NCI/NIH RO1 CA101904, P50 CA092131, NEI/ NIH RO1 EY017392) and the University of California at Berkeley.

REFERENCES

1. Chen L. Ocular lymphatics: State-of-the-art review. Lymphology. 2009; 42:66–76. [PubMed: 19725271]
2. Alitalo K, Tammela T, Petrova TV. Lymphangiogenesis in development and human disease. Nature. 2005; 438:946–953. [PubMed: 16355212]
3. Brown P. Lymphatic system: Unlocking the drains. Nature. 2005; 436:456–458. [PubMed: 16049446]
4. Jackson DG. The lymphatics revisited: New perspectives from the hyaluronan receptor LYVE-1. Trends Cardiovasc Med. 2003; 13:1–7. [PubMed: 12554094]
5. Chang L, Kaipainen A, Folkman J. Lymphangiogenesis new mechanisms. Ann N Y Acad Sci. 2002; 979:111–119. [PubMed: 12543721]
6. Folkman J, Kaipainen A. Genes tell lymphatics to sprout or not. Nat Immunol. 2004; 5:11–12. [PubMed: 14699399]
7. Oliver G, Detmar M. The rediscovery of the lymphatic system: Old and new insights into the development and biological function of the lymphatic vasculature. Genes Dev. 2002; 16:773–783. [PubMed: 11937485]
8. Collin HB. Endothelial cell lined lymphatics in the vascularized rabbit cornea. Invest Ophthalmol. 1966; 5:337–354. [PubMed: 5912539]
9. Collin HB. Ultrastructure of lymphatic vessels in the vascularized rabbit cornea. Exp Eye Res. 1970; 10:207–213. [PubMed: 5484764]
10. Cursiefen C, Chen L, Dana MR, et al. Corneal lymphangiogenesis: Evidence, mechanisms, and implications for corneal transplant immunology. Cornea. 2003; 22:273–281. [PubMed: 12658100]
11. Chen L, Cursiefen C, Barabino S, et al. Novel expression and characterization of lymphatic vessel endothelial hyaluronate receptor 1 (LYVE-1) by conjunctival cells. Invest Ophthalmol Vis Sci. 2005; 46:4536–4540. [PubMed: 16303945]
12. Cheng WS, Kraaij R, Nilsson B, et al. A novel TARP-promoterbased adenovirus against hormone-dependent and hormone-refractory prostate cancer. Mol Ther. 2004; 10:355–364. [PubMed: 15294182]
13. Chen L, Hamrah P, Cursiefen C, et al. Vascular endothelial growth factor receptor-3 mediates induction of corneal alloimmunity. Nat Med. 2004; 10:813–815. [PubMed: 15235599]

14. Cursiefen C, Chen L, Borges LP, et al. VEGF-A stimulates lymphangiogenesis and hemangiogenesis in inflammatory neovascularization via macrophage recruitment. J Clin Invest. 2004; 113:1040–1050. [PubMed: 15057311]
15. Ecoiffier TYD, Chen L. Differential distribution of blood and lymphatic vessels in the murine cornea. Invest Ophthalmol Vis Sci. 2010; 51:2436–2440. [PubMed: 20019372]
16. Folkman J. Tumor angiogenesis: Therapeutic implications. N Engl J Med. 1971; 285:1182–1186. [PubMed: 4938153]
17. Gimbrone MA Jr, Cotran RS, Leapman SB, et al. Tumor growth and neovascularization: An experimental model using the rabbit cornea. J Natl Cancer Inst. 1974; 52:413–427. [PubMed: 4816003]
18. Chang LK, Garcia-Cardena G, Farnebo F, et al. Dose-dependent response of FGF-2 for lymphangiogenesis. Proc Natl Acad Sci USA. 2004; 101:11658–11663. [PubMed: 15289610]
19. Ziche M, Morbidelli L. The corneal pocket assay. Methods Mol Biol. 2009; 467:319–329. [PubMed: 19301681]
20. Bjorndahl M, Cao R, Nissen LJ, et al. Insulin-like growth factors 1 and 2 induce lymphangiogenesis in vivo. Proc Natl Acad Sci USA. 2005; 102:15593–15598. [PubMed: 16230630]
21. Langer R, Folkman J. Polymers for the sustained release of proteins and other macromolecules. Nature. 1976; 263:797–800. [PubMed: 995197]
22. Loughman MS, Chatzistefanou K, Gonzalez EM, et al. Experimental corneal neovascularisation using sucralfate and basic Fibroblast growth factor. Aust N Z J Ophthalmol. 1996; 24:289–295. [PubMed: 8913136]
23. Rogers MS, Birsner AE, D'Amato RJ. The mouse cornea micropocket angiogenesis assay. Nat Protoc. 2007; 2:2545–2550. [PubMed: 17947997]
24. Junghans BM, Collin HB. Limbal lymphangiogenesis after corneal injury: An autoradiographic study. Curr Eye Res. 1989; 8:91–100. [PubMed: 2707040]
25. Ling S, Lin H, Liang L, et al. Development of new lymphatic vessels in alkali-burned corneas. Acta Ophthalmol. 2009; 87:315–322. [PubMed: 18811642]
26. Albuquerque RJ, Hayashi T, Cho WG, et al. Alternatively spliced vascular endothelial growth factor receptor-2 is an essential endogenous inhibitor of lymphatic vessel growth. Nat Med. 2009; 15:1023–1030. [PubMed: 19668192]
27. Chen L, Huq S, Gardner H, et al. Very late antigen 1 blockade markedly promotes survival of corneal allografts. Arch Ophthalmol. 2007; 125:783–788. [PubMed: 17562989]
28. Cursiefen C, Ikeda S, Nishina PM, et al. Spontaneous corneal hem-and lymphangiogenesis in mice with destrin-mutation depend on VEGFR3 signaling. Am J Pathol. 2005; 166:1367–1377. [PubMed: 15855638]
29. Liu Y, Hamrah P, Zhang Q, et al. Draining lymph nodes of corneal transplant hosts exhibit evidence for donor major histocompatibility complex (MHC) class II-positive dendritic cells derived from MHC class II-negative grafts. J Exp Med. 2002; 195:259–268. [PubMed: 11805152] 29 Liu Y, Hamrah P, Zhang Q, et al. Draining lymph nodes of corneal transplant hosts exhibit evidence for donor major histocompatibility complex (MHC) class II-positive dendritic cells derived from MHC class II-negative grafts. J Exp Med. 2002; 195:259–268. [PubMed: 11805152]
30. Yamagami S, Dana MR. The critical role of lymph nodes in corneal alloimmunization and graft rejection. Invest Ophthalmol Vis Sci. 2001; 42:1293–1298. [PubMed: 11328742]
31. Achen MG, McColl BK, Stacker SA. Focus on lymphangiogenesis in tumor metastasis. Cancer Cell. 2005; 7:121–127. [PubMed: 15710325]
32. Tammela T, Alitalo K. Lymphangiogenesis: Molecular mechanisms and future promise. Cell. 2010; 140:460–476. [PubMed: 20178740]
33. Harisinghani MG, Barentsz J, Hahn PF, et al. Noninvasive detection of clinically occult lymph-node metastases in prostate cancer. N Engl J Med. 2003; 348:2491–2499. [PubMed: 12815134]
34. Christofk HR, Vander Heiden MG, Harris MH, et al. The M2 splice isoform of pyruvate kinase is important for cancer metabolism and tumour growth. Nature. 2008; 452:230–233. [PubMed: 18337823]

35. Flier JS, Mueckler MM, Usher P, et al. Elevated levels of glucose transport and transporter messenger RNA are induced by ras or src oncogenes. Science. 1987; 235:1492–1495. [PubMed: 3103217]
36. Beyer T, Townsend DW, Brun T, et al. A combined PET/CT scanner for clinical oncology. J Nucl Med. 2000; 41:1369–1379. [PubMed: 10945530]
37. Liu IJ, Zafar MB, Lai YH, et al. Fluorodeoxyglucose positron emission tomography studies in diagnosis and staging of clinically organ-confined prostate cancer. Urology. 2001; 57:108–111. [PubMed: 11164153]
38. Shreve PD, Grossman HB, Gross MD, et al. Metastatic prostate cancer: Initial findings of PET with 2-deoxy-2-[F-18]fluoro-dglucose. Radiology. 1996; 199:751–756. [PubMed: 8638000]
39. Seltzer MA, Barbaric Z, Belldegrun A, et al. Comparison of helical computerized tomography, positron emission tomography and monoclonal antibody scans for evaluation of lymph node metastases in patients with prostate specific antigen relapse after treatment for localized prostate cancer. J Urol. 1999; 162:1322–1328. [PubMed: 10492189]
40. Larson SM, Morris M, Gunther I, et al. Tumor localization of 16beta-18F-fluoro-5alpha-dihydrotestosterone versus 18F-FDG in patients with progressive, metastatic prostate cancer. J Nucl Med. 2004; 45:366–373. [PubMed: 15001675]
41. Chen Y, Sawyers CL, Scher HI. Targeting the androgen receptor pathway in prostate cancer. Curr Opin Pharmacol. 2008; 8:440–448. [PubMed: 18674639]
42. DeGrado TR, Coleman RE, Wang S, et al. Synthesis and evaluation of 18F-labeled choline as an oncologic tracer for positron emission tomography: Initial findings in prostate cancer. Cancer Res. 2001; 61:110–117. [PubMed: 11196147]
43. Schuster DM, Votaw JR, Nieh PT, et al. Initial experience with the radiotracer anti-1-amino-3-18F-fluorocyclobutane-1-carboxylic acid with PET/CT in prostate carcinoma. J Nucl Med. 2007; 48:56–63. [PubMed: 17204699]
44. Picchio M, Messa C, Landoni C, et al. Value of [11C]cholinepositron emission tomography for re-staging prostate cancer: A comparison with [18F]fluorodeoxyglucose-positron emission tomography. J Urol. 2003; 169:1337–1340. [PubMed: 12629355]
45. Yamaguchi T, Lee J, Uemura H, et al. Prostate cancer: A comparative study of 11C-choline PET and MR imaging combined with proton MR spectroscopy. Eur J Nucl Med Mol Imaging. 2005; 32:742–748. [PubMed: 16052370]
46. Scattoni V, Picchio M, Suardi N, et al. Detection of lymph-node metastases with integrated [11C]choline PET/CT in patients with PSA failure after radical retropubic prostatectomy: Results confirmed by open pelvic-retroperitoneal lymphadenectomy. Eur Urol. 2007; 52:423–429. [PubMed: 17397992]
47. Rinnab L, Mottaghy FM, Simon J, et al. [11C]Choline PET/CT for targeted salvage lymph node dissection in patients with biochemical recurrence after primary curative therapy for prostate cancer. Preliminary results of a prospective study. Urol Int. 2008; 81:191–197. [PubMed: 18758218]
48. Shu X, Royant A, Lin MZ, et al. Mammalian expression of infrared fluorescent proteins engineered from a bacterial phytochrome. Science. 2009; 324:804–807. [PubMed: 19423828]
49. Gambhir SS, Bauer E, Black ME, et al. A mutant herpes simplex virus type 1 thymidine kinase reporter gene shows improved sensitivity for imaging reporter gene expression with positron emission tomography. Proc Natl Acad Sci USA. 2000; 97:2785–2790. [PubMed: 10716999]
50. Groot-Wassink T, Aboagye EO, Glaser M, et al. Adenovirus biodistribution and noninvasive imaging of gene expression in vivo by positron emission tomography using human sodium/ iodide symporter as reporter gene. Hum Gene Ther. 2002; 13:1723–1735. [PubMed: 12396625]
51. Rogers BE, Chaudhuri TR, Reynolds PN, et al. Non-invasive gamma camera imaging of gene transfer using an adenoviral vector encoding an epitope-tagged receptor as a reporter. Gene Ther. 2003; 10:105–114. [PubMed: 12571639]
52. Massoud TF, Gambhir SS. Molecular imaging in living subjects: Seeing fundamental biological processes in a new light. Genes Dev. 2003; 17:545–580. [PubMed: 12629038]
53. Singh A, Massoud TF, Deroose C, et al. Molecular imaging of reporter gene expression in prostate cancer: An overview. Semin Nucl Med. 2008; 38:9–19. [PubMed: 18096460]

54. Kang JH, Chung JK. Molecular-genetic imaging based on reporter gene expression. J Nucl Med. 2008; 49:164S–179S. [PubMed: 18523072]
55. Gambhir, SS. Molecular imaging with reporter genes. Cambridge: Cambridge University Press; 2010.
56. Figueiredo ML, Kao C, Wu L. Advances in preclinical investigation of prostate cancer gene therapy. Mol Ther. 2007; 15:1053–1064. [PubMed: 17457317]
57. Adams JY, Johnson M, Sato M, et al. Visualization of advanced human prostate cancer lesions in living mice by a targeted gene transfer vector and optical imaging. Nat Med. 2002; 8:891–897. [PubMed: 12134144]
58. Latham JP, Searle PF, Mautner V, et al. Prostate-specific antigen promoter/enhancer driven gene therapy for prostate cancer: Construction and testing of a tissue-specific adenovirus vector. Cancer Res. 2000; 60:334–341. [PubMed: 10667585]
59. Yu DC, Sakamoto GT, Henderson DR. Identification of the transcriptional regulatory sequences of human kallikrein 2 and their use in the construction of calydon virus 764, an attenuated replication competent adenovirus for prostate cancer therapy. Cancer Res. 1999; 59:1498–1504. [PubMed: 10197620]
60. Zhang Y, Yu J, Unni E, et al. Monogene and polygene therapy for the treatment of experimental prostate cancers by use of apoptotic genes bax and bad driven by the prostate-specific promoter ARR(2)PB. Hum Gene Ther. 2002; 13:2051–2064. [PubMed: 12490000]
61. Lee SJ, Zhang Y, Lee SD, et al. Targeting prostate cancer with conditionally replicative adenovirus using PSMA enhancer. Mol Ther. 2004; 10:1051–1058. [PubMed: 15564137]
62. Iyer M, Wu L, Carey M, et al. Two-step transcriptional amplification as a method for imaging reporter gene expression using weak promoters. Proc Natl Acad Sci USA. 2001; 98:14595–14600. [PubMed: 11734653]
63. Zhang L, Adams JY, Billick E, et al. Molecular engineering of a two-step transcription amplification (TSTA) system for transgene delivery in prostate cancer. Mol Ther. 2002; 5:223–232. [PubMed: 11863411]
64. Sato M, Johnson M, Zhang L, et al. Functionality of androgen receptor-based gene expression imaging in hormone refractory prostate cancer. Clin Cancer Res. 2005; 11:3743–3749. [PubMed: 15897571]
65. Johnson M, Sato M, Burton J, et al. Micro-PET/CT monitoring of herpes thymidine kinase suicide gene therapy in a prostate cancer xenograft: The advantage of a cell-specific transcriptional targeting approach. Mol Imaging. 2005; 4:463–472. [PubMed: 16285908]
66. Ray S, Paulmurugan R, Patel MR, et al. Noninvasive imaging of therapeutic gene expression using a bidirectional transcriptional amplification strategy. Mol Ther. 2008; 16:1848–1856. [PubMed: 18766175]
67. Huyn ST, Burton JB, Sato M, et al. A potent, imaging adenoviral vector driven by the cancer-selective mucin-1 promoter that targets breast cancer metastasis. Clin Cancer Res. 2009; 15:3126–3134. [PubMed: 19366829]
68. Chen IY, Gheysens O, Ray S, et al. Indirect imaging of cardiac-specific transgene expression using a bidirectional two-step transcriptional amplification strategy. Gene Ther. 2010; 17:827–838. [PubMed: 20237511]
69. Szuba A, Shin WS, Strauss HW, et al. The third circulation: Radionuclide lymphoscintigraphy in the evaluation of lymphedema. J Nucl Med. 2003; 44:43–57. [PubMed: 12515876]
70. Ikomi F, Hanna GK, Schmid-Schonbein GW. Size-and surface-dependent uptake of colloid particles into the lymphatic system. Lymphology. 1999; 32:90–102. [PubMed: 10494521]
71. Ikomi F, Hanna GK, Schmid-Schonbein GW. Mechanism of colloidal particle uptake into the lymphatic system: Basic study with percutaneous lymphography. Radiology. 1995; 196:107–113. [PubMed: 7784553]
72. Giuliano AE, Kirgan DM, Guenther JM, et al. Lymphatic mapping and sentinel lymphadenectomy for breast cancer. Ann Surg. 1994; 220:391–398. discussion 8-401. [PubMed: 8092905]
73. Gervasi LA, Mata J, Easley JD, et al. Prognostic significance of lymph nodal metastases in prostate cancer. J Urol. 1989; 142:332–336. [PubMed: 2501518]

74. Roehl KA, Han M, Ramos CG, et al. Cancer progression and survival rates following anatomical radical retropubic prostatectomy in 3,478 consecutive patients: Long-term results. J Urol. 2004; 172:910–914. [PubMed: 15310996]
75. Masterson TA, Bianco FJ Jr, Vickers AJ, et al. The association between total and positive lymph node counts, and disease progression in clinically localized prostate cancer. J Urol. 2006; 175:1320–1324. discussion 1324–1325. [PubMed: 16515989]
76. Zeng Y, Opeskin K, Baldwin ME, et al. Expression of vascular endothelial growth factor receptor-3 by lymphatic endothelial cells is associated with lymph node metastasis in prostate cancer. Clin Cancer Res. 2004; 10:5137–5144. [PubMed: 15297417]
77. Jennbacken K, Vallbo C, Wang W, et al. Expression of vascular endothelial growth factor C (VEGF-C) and VEGF receptor-3 in human prostate cancer is associated with regional lymph node metastasis. Prostate. 2005; 65:110–116. [PubMed: 15880525]
78. Brakenhielm E, Burton JB, Johnson M, et al. Modulating metastasis by a lymphangiogenic switch in prostate cancer. Int J Cancer. 2007; 121:2153–2161. [PubMed: 17583576]
79. Burton JB, Priceman SJ, Sung JL, et al. Suppression of prostate cancer nodal and systemic metastasis by blockade of the lymphangiogenic axis. Cancer Res. 2008; 68:7828–7837. [PubMed: 18829538]
80. Mattei A, Fuechsel FG, Bhatta Dhar N, et al. The template of the primary lymphatic landing sites of the prostate should be revisited: Results of a multimodality mapping study. Eur Urol. 2008; 53:118–125. [PubMed: 17709171]
81. Heidenreich A, Ohlmann CH, Polyakov S. Anatomical extent of pelvic lymphadenectomy in patients undergoing radical prostatectomy. Eur Urol. 2007; 52:29–37. [PubMed: 17448592]
82. Labow D, Lee S, Ginsberg RJ, et al. Adenovirus vector-mediated gene transfer to regional lymph nodes. Hum Gene Ther. 2000; 11:759–769. [PubMed: 10757355]
83. Johnson M, Huyn S, Burton J, et al. Differential biodistribution of adenoviral vector in vivo as monitored by bioluminescence imaging and quantitative polymerase chain reaction. Hum Gene Ther. 2006; 17:1262–1269. [PubMed: 17117891]
84. Kishimoto H, Kojima T, Watanabe Y, et al. In vivo imaging of lymph node metastasis with telomerase-specific replication-selective adenovirus. Nat Med. 2006; 12:1213–1219. [PubMed: 17013385]
85. Burton JB, Johnson M, Sato M, et al. Adenovirus-mediated gene expression imaging to directly detect sentinel lymph node metastasis of prostate cancer. Nat Med. 2008; 14:882–888. [PubMed: 18622403]
86. Kishimoto H, Urata Y, Tanaka N, et al. Selective metastatic tumor labeling with green fluorescent protein and killing by systemic administration of telomerase-dependent adenoviruses. Mol Cancer Ther. 2009; 8:3001–3008. [PubMed: 19887549]
87. Sato M, Figueiredo ML, Burton JB, et al. Configurations of a two-tiered amplified gene expression system in adenoviral vectors designed to improve the specificity of in vivo prostate cancer imaging. Gene Ther. 2008; 15:583–593. [PubMed: 18305574]
88. Penuelas I, Mazzolini G, Boan JF, et al. Positron emission tomography imaging of adenoviral-mediated transgene expression in liver cancer patients. Gastroenterology. 2005; 128:1787–1795. [PubMed: 15940613]
89. Barton KN, Stricker H, Brown SL, et al. Phase I study of noninvasive imaging of adenovirus-mediated gene expression in the human prostate. Mol Ther. 2008; 16:1761–1769. [PubMed: 18714306]
90. Liu H, Jin L, Koh SBS, et al. Atomic structure of human adenovirus by cryoEM reveals networks of protein interactions. Science. 2010; 329:1038–1043. [PubMed: 20798312]
91. Waddington SN, McVey JH, Bhella D, et al. Adenovirus serotype 5 hexon mediates liver gene transfer. Cell. 2008; 132:397–409. [PubMed: 18267072]
92. Roberts DM, Nanda A, Havenga MJ, et al. Hexon-chimaeric adenovirus serotype 5 vectors circumvent pre-existing anti-vector immunity. Nature. 2006; 441:239–243. [PubMed: 16625206]
93. Everts M, Curiel DT. Transductional targeting of adenoviral cancer gene therapy. Curr Gene Ther. 2004; 4:337–346. [PubMed: 15384947]

94. Ntziachristos V, Bremer C, Weissleder R. Fluorescence imaging with near-infrared light: New technological advances that enable in vivo molecular imaging. Eur Radiol. 2003; 13:195–208. [PubMed: 12541130]

95. Edinger M, Cao YA, Hornig YS, et al. Advancing animal models of neoplasia through in vivo bioluminescence imaging. Eur J Cancer. 2002; 38:2128–2136. [PubMed: 12387838]

96. MacLaren DC, Gambhir SS, Satyamurthy N, et al. Repetitive, non-invasive imaging of the dopamine D2 receptor as a reporter gene in living animals. Gene Ther. 1996; 6:785–791. [PubMed: 10505102]

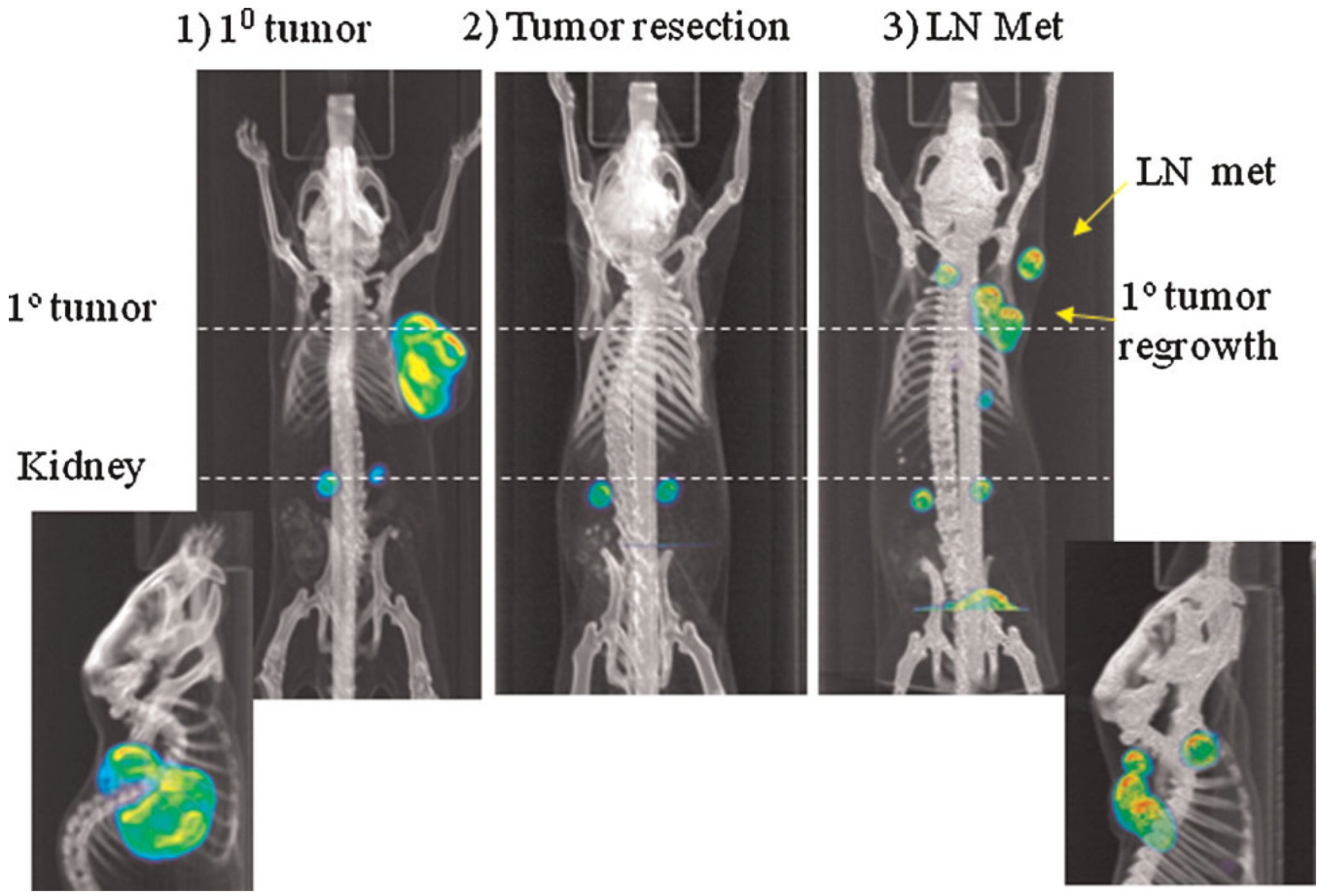

Fig. 1.

18F-FLT PET–CT to monitor tumor growth and LN metastasis. Subcutaneous LAPC-9 tumor was visualized using 18F-FLTat 4 week after tumor implantation (1, coronal view, with sagittal view of the tumor shown below). At this time point, primary tumor was resected (2). 21 days after tumor resection (3), FLT-PET showed primary tumor regrowth and dissemination to regional LN (yellow arrows), a sagittal view was shown below. [Color figure can be viewed in the online issue, available at wileyonlinelibrary.com.]

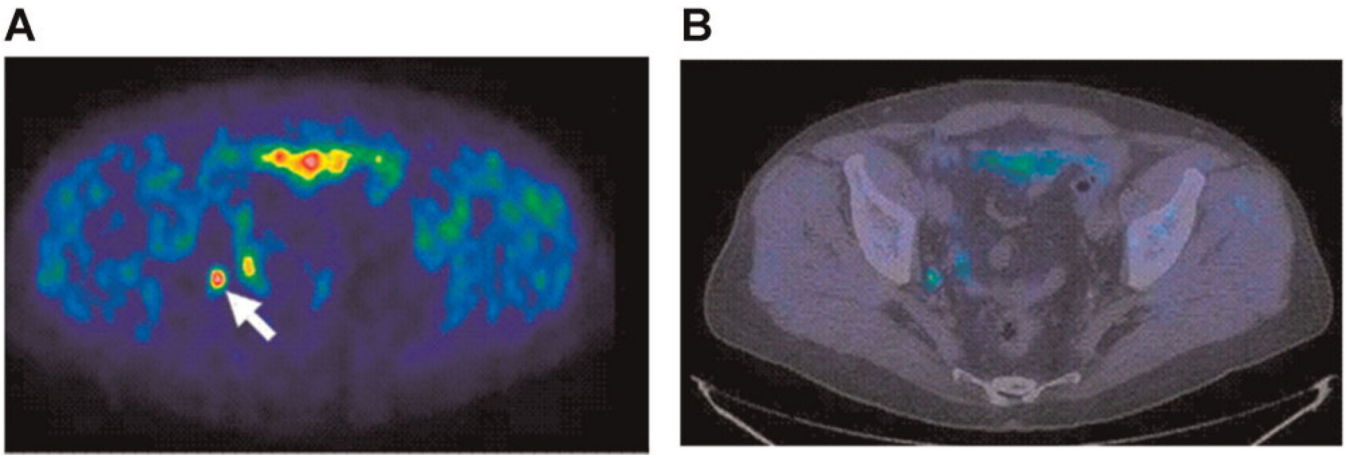

Fig. 2.

PET–CT to detect prostate cancer lymph node metastasis. ^{11}C-Choline PET–CT in a patient with PSA recurrence after radical prostatectomy. PET transaxial image at pelvis level (A) shows an increased [^{11}C]choline uptake (SUV ¼ 2.5), corresponding to a lymph node of the right internal iliac chain (arrow), as shown in the combined PET/CT corresponding image (B). Histopathology after surgical resection confirmed the presence of viable tumor cells in the lymph node. PET, positron emission tomography; SUV, standardized uptake value; CT, computed tomography. Adapted from Scattoni et al. [46], reprinted with permission from Elsevier. [Color figure can be viewed in the online issue, available at wileyonlinelibrary.com.]

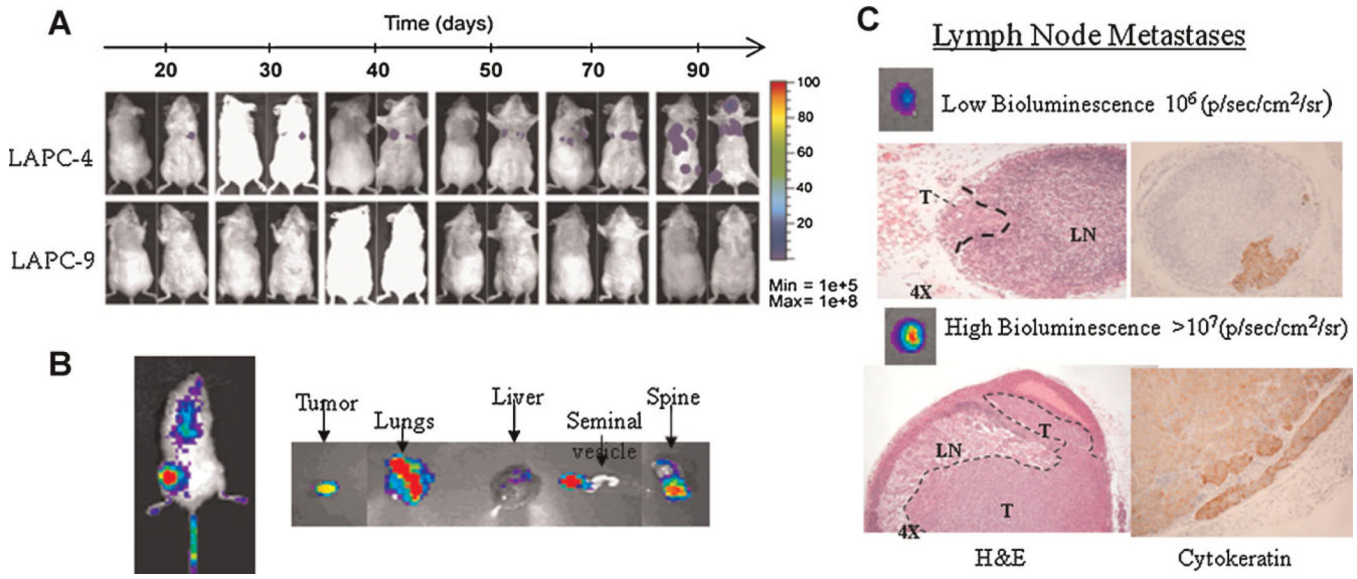

Fig. 3.

Bioluminescence imaging (BLI) to study experimental metastasis. A: The use of BLI to assess metastatic potentials of two prostate xenograft models (LAPC-4 and -9), longitudinal over time. The ease of use and low background of luciferase reporter genes are clear advantages.

B: BLI provides a 2-D semi-quantitative signal, which is difficult to localize in a metastatic setting. Imaging of harvested organs ex vivo can aid in analyze the magnitude and localization of tumor spread. C: The magnitude of bioluminescence signals in isolated organs correlates well with volume of metastasis, as assayed in the lymph node metastasis. These results are adapted from Brakenhielm et al. [78]. [Color figure can be viewed in the online issue, available at wileyonlinelibrary.com.]

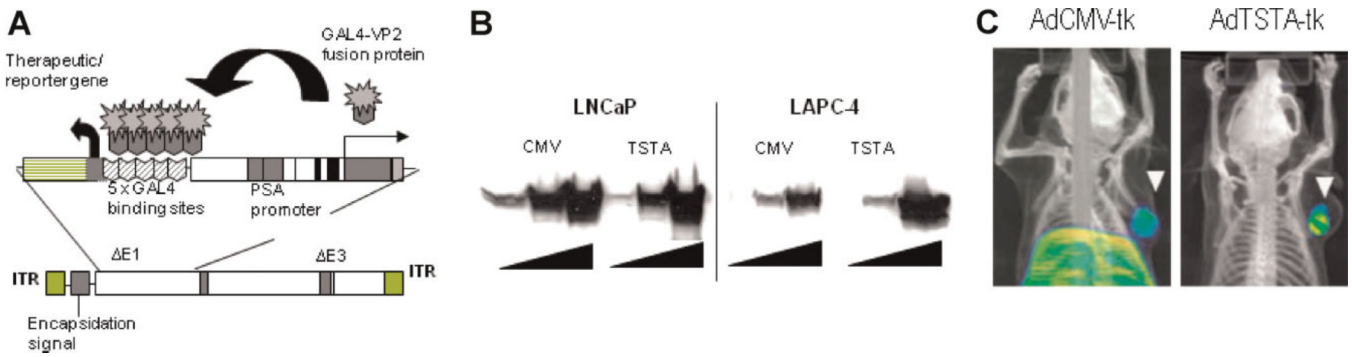

Fig. 4.

Amplified prostate-specific HSV-tk imaging vector. A: The Ad containing the TSTA system. The enhanced prostate-specific PSA promoter drives the expression of the potent synthetic activator, composed of 2 herpes VP16 activation domains (aa 413–454) fused to the GAL4 DNA binding domain. The GAL4-VP2 activators bind to the GAL4 binding sites, activating the expression of the HSV-tk gene. These two components were inserted into the E1 genome region of an Ad5 vector. B: The magnitude of HSV1-tk expression. LNCaP and LAPC-4 prostate cancer cells were infected with increasing dose strong constitutive AdCMV-tk or prostate-specific AdTSTA-tk at MOI 0.2, 1, and 5 (triangle). The level of HSV1-tk protein expression as assessed by Western blot was quite comparable between the two vectors. C: Prostate-restricted expression of AdTSTA-tk. Intratumoral injection of both AdCMV-tk and AdTSTA-tk resulted in visible tumor signal in the tumor (white arrowhead). But the constitutive AdCMV-tk also resulted in strong PET signal in the liver, due to systemic leakage of vector. Gene delivery to the tumor and liver by AdTSTA-tk was comparable to AdCMV-tk as demonstrated by PCR (data not shown). But the prostate-specific TSTA system prevented the unintended expression in the liver (Johnson et al. [65]). [Color figure can be viewed in the online issue, available at wileyonlinelibrary.com.]

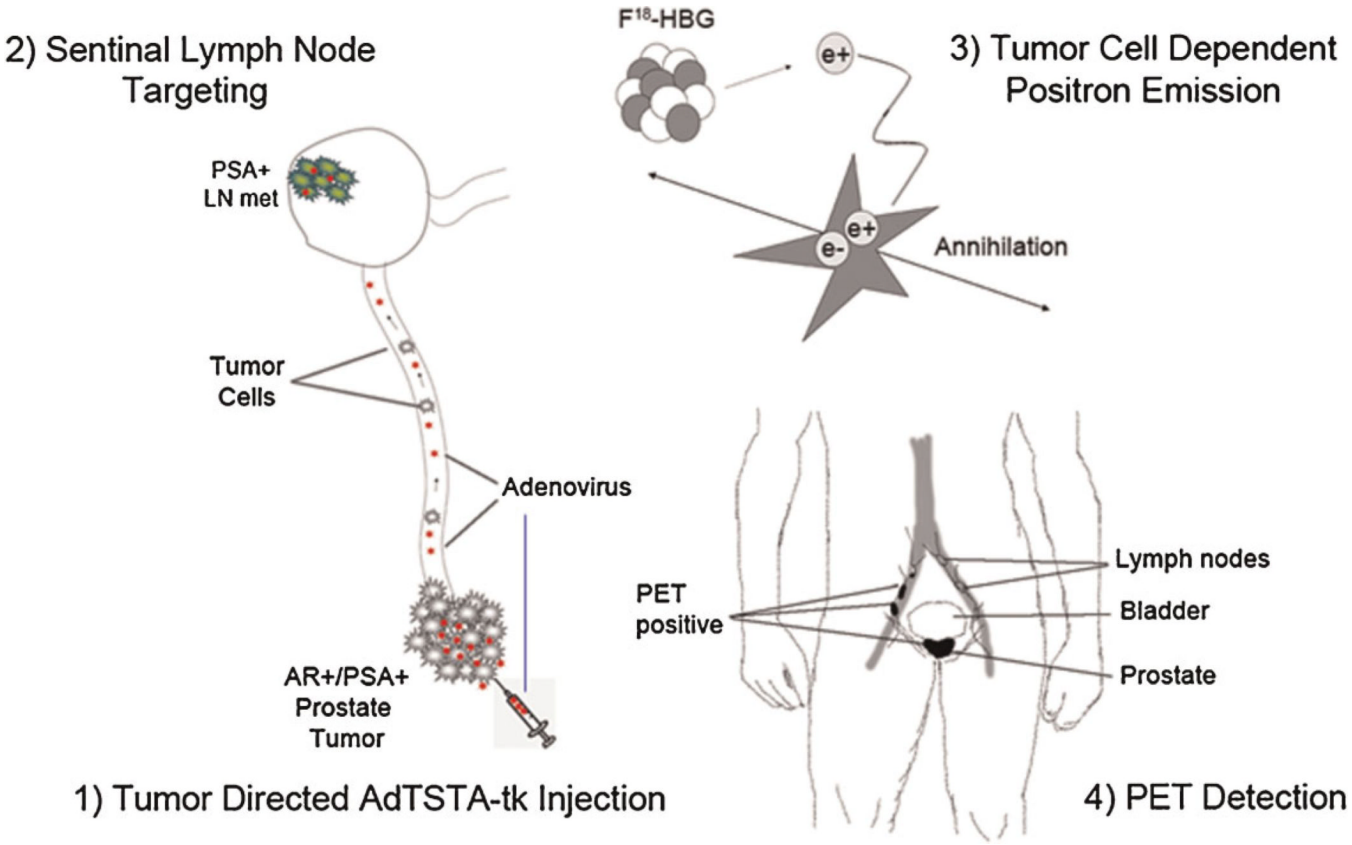

Fig. 5.

Ad lymphangiography method to identify prostate nodal metastasis based on gene expression. Steps for the potential clinical application of Ad-mediated detection of sentinel lymph node metastasis. 1: Tumor interstitial directed AdTSTA-sr39tk injection. 2: SLN targeting: In contrast to colloid-mediated lymphoscintigraphy, Ad can transduce tumor cells within LNs. 3: Tumor cell dependent positron emission. The gene expression control incorporated into the Ad restricts the expression of the imaging reporter gene (thymidine kinase, sr39tk) to PSAþ/ARþprostate cancer cells. The expression of sr39tk leads to the trapping of 18F-HBG tracer in tumor cells in the metastatic sentinel nodes. 4: PET detection: The 18F-FHBG positron signals accumulated in tumor cells will be detected by high-resolution PET/CT. [Color figure can be viewed in the online issue, available at wileyonlinelibrary.com.]

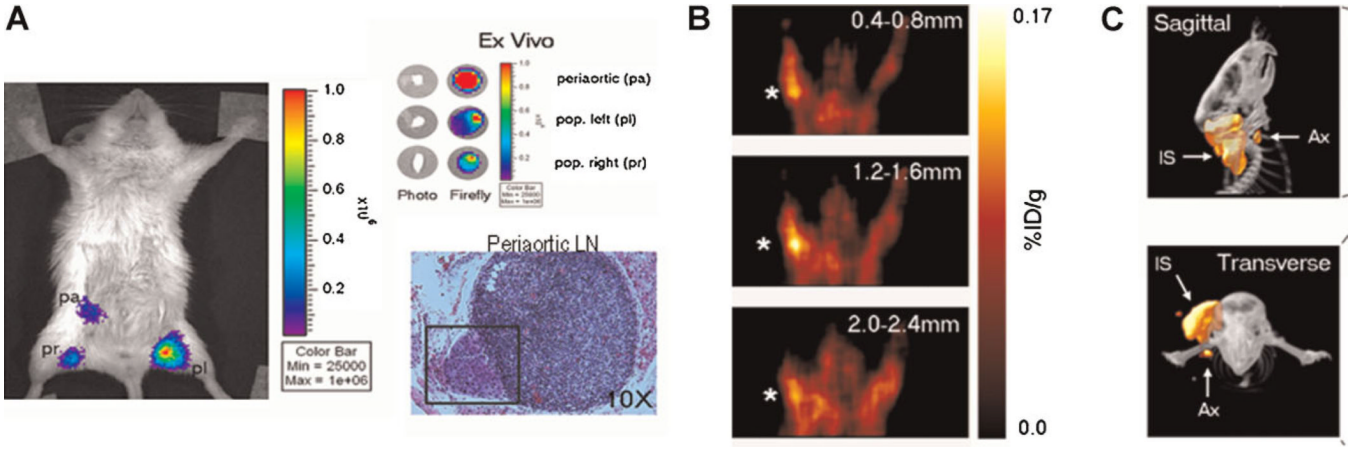

Fig. 6.

Prostate-specific TSTA Ad detection of lymph node metastases of prostate cancer. A: Firefly luciferase expressing AdTSTA-fl was injected in both hind paws of an animal harboring an orthotopic human prostate tumor (LAPC9/VEGF-C). Ex vivo imaging of the harvested pelvic nodes indicated that the largest volume of metastasis was located in the periaortic lymph node, as noted by its signal intensity. Histology (H&E) revealed a small subcapsular lesion (marked by a square) within this periaortic node. The number of cells detected within the node metastases was estimated to be ~4×10^3 cells. B: AdTSTA-tk virus was injected into both front paws of an animal bearing LAPC9/VEGF-C tumor grafted in right upper back. Positive FHBG-PET signal was detected in the tumor cell-positive axillary lymph node, ipsilateral (star) but not contralateral to the tumor. C: Detection of occult lymph node metastasis by microPET/CT imaging. A mouse bearing a tumor with nodal metastasis received AdTSTA-tk via intratumoral injections. The hypothesis tested was that Ad could drain out of the tumor through peritumoral lymphatic vessels and into the regional sentinel lymph nodes. Signals were detected in both the tumor and the draining sentinel lymph node using ^{18}FHBG PET imaging. Representative sagittal (top) and transverse (bottom) microPET/CT images show that PET signal is emitted from the tumor injection site (IS) as well as the draining axillary sentinel lymph nodes (Ax). Images adapted with permission from Burton et al. [85]. [Color figure can be viewed in the online issue, available at wileyonlinelibrary.com.]

TABLE 1

Common Imaging Reporter Genes Used in Cancer Research

Imaging modality	Reporter gene	Probe/substrate	Applications
Optical imaging	Fluorescent proteins: GFP, RFP, IFP	None	Cellular and microscopic imaging; IR better for spectral in vivo imaging [48,94]
	Bioluminescence proteins: luciferases (firefly, renilla, gaussia)	D-Luciferin, coelenterazine	Cell marking, small animal in vivo imaging [95]

The imaging modality, probe and or substrate and application suited for a particular reporter gene is listed. In general, optical imaging approaches are more suitable for cellular and small animal imaging, while radionuclide imaging can be used in both preclinical and clinical settings.